Journal of Power Sources 239 (2013) 265–268

Contents lists available at SciVerse ScienceDirect

Journal of Power Sources

journal homepage: www.elsevier.com/locate/jpowsour

Short communication

The electrochemical behaviors of Mg–8Li–0.5Y and Mg–8Li–1Y alloys in sodium chloride solution

Yanzhuo Lv [a,*], Min Liu [a], Yan Xu [b], Dianxue Cao [a], Jing Feng [a], Ruizhi Wu [a], Milin Zhang [a]

[a] The College of Material Science and Chemical Engineering, Harbin Engineering University, Harbin 150001, PR China
[b] The College of Mechanical and Electrical Engineering, Harbin Engineering University, Harbin 150001, PR China

HIGHLIGHTS

- The Mg–Li–Y is a new material that has been studied as the anode of Mg–H_2O_2 semi-fuel cells.
- The novel alloys would be the more excellent anodes than Mg in Mg–H_2O_2 semi-fuel cells.
- Modifying the Y content can alter the performance of the Mg–Li–Y alloy as the anode material.

ARTICLE INFO

Article history:
Received 9 January 2013
Received in revised form
16 March 2013
Accepted 20 March 2013
Available online 1 April 2013

Keywords:
Magnesium–lithium-based alloys
Electrochemical performances
Anode material
Magnesium–hydrogen peroxide semi-fuel cells

ABSTRACT

The electrochemical performances of Mg–8Li–0.5Y and Mg–8Li–1Y electrodes in 0.7 mol L^{-1} NaCl solution are investigated by methods of potentiodynamic polarization, electrochemical impedance spectroscopy, potentiostatic oxidation and scanning electron microscopy (SEM). Their performances as anodes of Mg–H_2O_2 semi-fuel cells are also determined. It is found that the Mg–8Li–1Y electrode has higher corrosion resistant ability and electrooxidation activity than that of Mg–8Li–0.5Y electrode in 0.7 mol L^{-1} NaCl solution. The corrosion potential of Mg–8Li–1Y electrode is 60 mV more positive than that of Mg–8Li–0.5Y electrode. The current density of Mg–8Li–1Y electrode is around 2 mA cm^{-2} higher than that of Mg–8Li–0.5Y electrode at the discharge potentials of −0.8 V, −1.0 V and −1.2 V, and it is similar to that of Mg–8Li–0.5Y electrode at −1.4 V. The Mg–H_2O_2 semi-fuel cell with Mg–8Li–1Y anode presents a maximum power density of 59 mW cm^{-2} at room temperature, which is higher than that of Mg–8Li–0.5Y anode (53 mW cm^{-2}). The content of Y in alloys obviously affects the performance of the alloys and the Y content of 1 wt. % is better than 0.5 wt. %.

1. Introduction

The aluminum metal as the anode of metal–hydrogen peroxide semi-fuel cell has been studied extensively. However, the theoretical cell potential of magnesium–hydrogen peroxide (Mg–H_2O_2) electrochemical system is 4.14 V, which is higher than that of the aluminum–hydrogen peroxide semi-fuel cell [1]. In addition, magnesium and magnesium alloys as anodes of magnesium–hydrogen peroxide semi-fuel cell systems have the advantages of high Faradic capacity, high specific energy, more negative standard electroreduction potentials, and high discharge performances in seawater electrolyte [2–10]. Therefore, Mg–H_2O_2 semi-fuel cells have been developed as power sources for low rate, long endurance autonomous underwater vehicle (AUV) in Naval Undersea Warfare Center and University of Massachusetts [2,3].

In practical application, magnesium alloy electrodes operate at significantly less negative potential mainly due to the passive oxide films on the magnesium alloy surface, which cause a delay in reaching a steady-state and a reduction in discharging rate [11]. Song et al. [12] reported that a loose and uneven layer of hydroxyl or oxide protective coating is usually formed on Mg–Li alloy surface in air or neutral environment. It can not provide a good protection for Mg–Li alloys. In addition, magnesium alloy undergoes parasitic corrosion reactions or self-discharge, resulting in the reduction of Coulombic efficiency and the evolution of hydrogen [11,13]. To overcome these problems, doping the magnesium alloy with other alloying elements has been investigated [14]. The alloying elements, such as aluminum, zinc, silver, silicon, cadmium and rare earth (RE), are introduced to improve the electrochemical behaviors of Mg–Li binary alloys. Cao et al. [11,13,15] reported that Mg–Li-based alloys, such as Mg–Li, Mg–Li–Al, Mg–Li–Al–Ce, Mg–Li–

* Corresponding author. Tel.: +86 13845079693.
E-mail address: lvyanzhuo@hrbeu.edu.cn (Y. Lv).

0378-7753/$ – see front matter © 2013 Elsevier B.V. All rights reserved.
http://dx.doi.org/10.1016/j.jpowsour.2013.03.112

Al–Sn, Mg–Li–Al–Ce–Sn, Mg–Li–Al–Ce–Zn, and Mg–Li–Al–Ce–Zn–Mn, exhibited high electrooxidation activity in 0.7 mol L^{-1} NaCl solution. Our group [17] found that Mg–Li–Al–Ce–Y electrode is more corrosion resistive than that of Mg–Li–Al–Ce electrode. Y can change the alloy structure or assist the formation of an easy-peel off layer on the alloys surface. We [18] also demonstrated that Mg–8Li–3Al–0.5Zn electrode has higher discharge activity and less corrosion resistance than Mg–8Li–3Al–1.0Zn electrode. The content of Zn in the alloys obviously affected the alloy performances and the Zn content of 0.5 wt. % is better than 1 wt. %.

This work seeks to study the effects of Y content on the electrochemical behaviors of bimetallic Mg–8Li alloys. Mg–8Li–0.5Y and Mg–8Li–1Y alloys were prepared and their electrochemical behaviors in 0.7 mol L^{-1} NaCl solution were investigated. The performances of Mg–H_2O_2 semi-fuel cells using the above metal anodes were also examined.

2. Experimental

All chemicals were of reagent grade and used as obtained from the supplier without further purification. All solutions were prepared using deionized water.

2.1. Preparation of Mg–Li-based alloys

Mg–8Li–0.5Y and Mg–8Li–1Y alloys were prepared in a vacuum electromagnetic induction melting furnace under the ambient of argon gas. The metals for the alloys preparation were pure magnesium (99.90 wt. %), pure lithium (99.90 wt. %), and Mg–Y alloy with 25.67 wt. % Y. The induction furnace is connected to an AC power source. The alloying components were charged into the induction furnace, which was then evacuated to 1.0×10^{-2} Pa and heated to 700 °C to melt the metal components. The formed molten alloy was then poured into a stainless steel mold and cooled down to ambient temperature under argon atmosphere in the furnace within 2 h. The nominal compositions of the alloys are given in Table 1.

The alloy ingots were machined to 20 mm × 20 mm × 2 mm. Prior to each experiment, the sample was successively polished with SiC abrasive papers to 600 grit and 2000 grit, washed with deoxygenated ultrapure water (Milli-Q), degreased with acetone and rinsed with deoxygenated ultrapure water again, and then immediately assembled into the electrochemical cell.

2.2. Electrochemical measurements

In the electrochemical measurements, a specifically designed home-made three-electrode electrochemical cell [17] was used. The cell was equipped with a platinum counter electrode, a saturated calomel reference electrode (SCE), and the Mg–8Li–0.5Y or Mg–8Li–1Y alloy working electrode. The exposure area of the metal alloy electrode is 0.5024 cm^2, which was used to calculate the current density. Electrochemical experiments were carried out in 0.7 mol L^{-1} NaCl aqueous solution at room temperature. The solution was purged with N_2 gas for 15 min before measurements in order to remove the dissolved O_2. Electrochemical measurement techniques included potentiodynamic polarization (5 mV s^{-1}, −2.2 V to −0.8 V), electrochemical impedance spectroscopy (0.1–10^5 Hz, 5 mV, at the corrosion potential determined by the potentiodynamic polarization), potentiostatic oxidation (15 min, −1.0 V). Scanning electron microscopy (SEM: S4800; JSM-6480) was used to observe the surface morphology after the samples were consecutively discharged at −1.4, −1.2, −1.0 and −0.8 V each for 15 min in 0.7 mol L^{-1} NaCl solution.

Table 1
Chemical compositions of alloys (wt.%).

Alloys	Mg	Li	Y
Mg–8Li–0.5Y	91.5	8	0.5
Mg–8Li–1Y	91	8	1

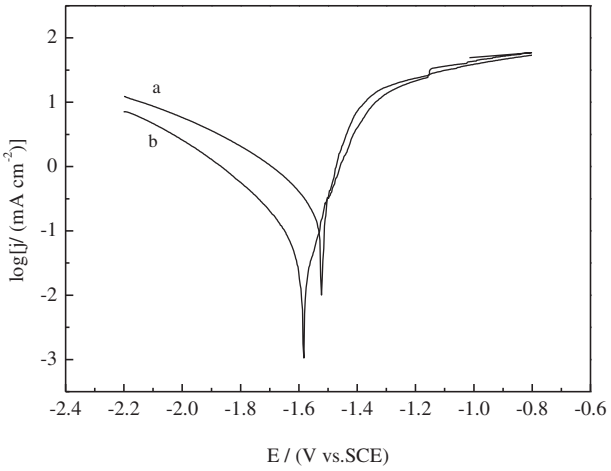

Fig. 1. Potentiodynamic polarization curves for (a) Mg–8Li–0.5Y and (b) Mg–8Li–1Y electrodes measured in 0.7 mol L^{-1} NaCl solution. Scan rate: 5 mV s^{-1}.

2.3. Magnesium–hydrogen peroxide semi-fuel cell tests

The performances of the magnesium–hydrogen peroxide semi-fuel cells depend on parameters such as: the concentration of H_2O_2 in the catholyte, the cell temperature, the catholyte flow rate, and the anolyte flow rate. A home-made flow through test cell made of Plexiglas was used. The Mg–Li-based alloys were used as the anode and the Au coated nickel foam served as the cathode. The area of the cathode was 2.25 cm^2 (15 mm × 15 mm). Nafion-115 membrane was used to separate the anode and the cathode compartments. The anolyte (0.7 mol L^{-1} NaCl) and the catholyte (0.7 mol L^{-1} NaCl + 0.1 mol L^{-1} H_2SO_4 + 0.5 mol L^{-1} H_2O_2) were pumped into the bottom of the anode and the cathode compartments, respectively, and exited at the top of the compartments. The flow rates of both the anolyte and the catholyte were 85 mL min^{-1}, which were controlled by individual peristaltic pump.

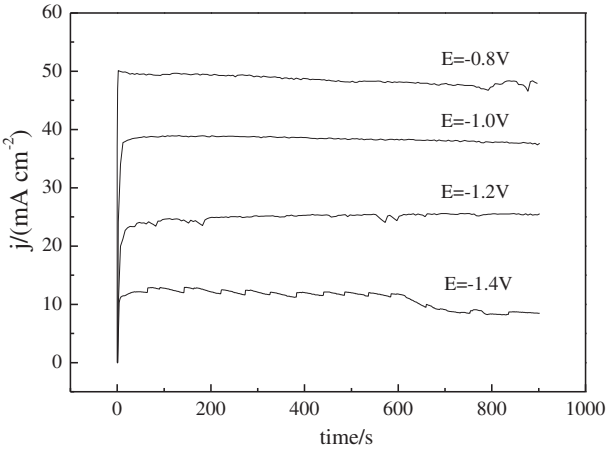

Fig. 2. Current–time curves for Mg–8Li–0.5Y recorded in 0.7 mol L^{-1} NaCl solution at various anodic potentials.

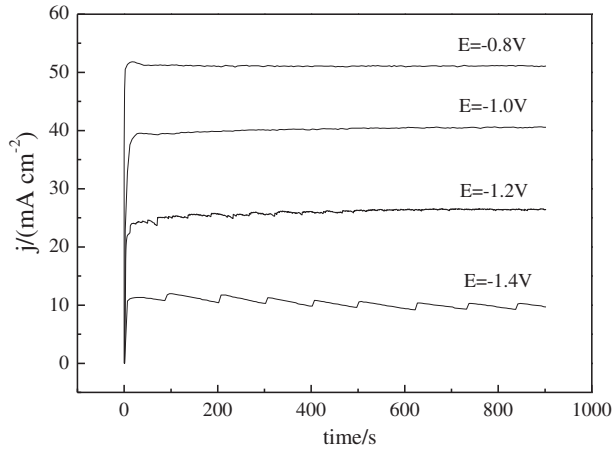

Fig. 3. Current–time curves for Mg–8Li–1Y recorded in 0.7 mol L^{-1} NaCl solution at various anodic potentials.

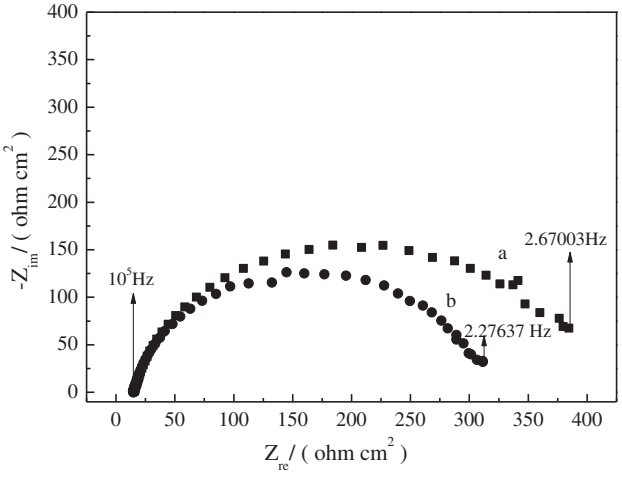

Fig. 4. The impedance spectra of (a) Mg–8Li–0.5Y and (b) Mg–8Li–1Y electrodes recorded in 0.7 mol L^{-1} NaCl solution.

3. Results and discussion

3.1. Potentiodynamic polarization

Fig. 1 shows the potentiodynamic polarization curves of Mg–8Li–0.5Y and Mg–8Li–1Y electrodes measured in 0.7 mol L^{-1} NaCl solution at a scan rate of 5 mV s^{-1}. As seen, the corrosion potential of Mg–8Li–0.5Y electrode is −1.58 V, which is 50 mV more positive than that of pure Mg electrode (−1.63 V as we previously reported) [11,18,19], and 90 mV more positive than that of Mg–8Li electrode (−1.67 V as we previously reported) [11,20]. This result implies that Mg–8Li–0.5Y electrode is more corrosion resistant than pure Mg and Mg–8Li electrodes, which might be attributed to the presence of Y. The corrosion potential of Mg–8Li–1Y electrode is −1.52 V, which is 60 mV more positive than that of Mg–8Li–0.5Y electrode, indicating that Mg–8Li–1Y electrode is more corrosion resistant than Mg–8Li–0.5Y electrode.

3.2. Potentiostatic measurements

Figs. 2 and 3 show the discharge behaviors of Mg–8Li–0.5Y and Mg–8Li–1Y electrodes under different potentials (−0.8 V, −1.0 V, −1.2 V, −1.4 V) in 0.7 mol L^{-1} NaCl solution. Both samples displayed similar current–time curves, that is, the anodic current increased rapidly in the early discharging stage and then reached to an approximate constant value. The discharge current density of Mg–8Li–1Y electrode is around 2 mA cm^{-2} higher than that of Mg–8Li–0.5Y electrode at the discharge potentials of −0.8 V, −1.0 V and −1.2 V, and it is similar to that of Mg–8Li–0.5Y electrode at −1.4 V, indicating that Mg–8Li–1Y electrode is more electro-active than Mg–8Li–0.5Y electrode at anodic potentials higher than −1.4 V. The potentiostatic current–time measurements also lead to the conclusion that Mg–8Li–1Y electrode has higher discharge activity (41 mA cm^{-2}) than that of pure Mg electrode (38 mA cm^{-2}) [16] at −1.0 V. Cao et al. [11] reported that the discharging current density of Mg electrode is similar to that of the Mg–8Li electrode. So it can be concluded that the doping of Y element (0.5 wt. % and 1 wt. %) into the Mg–8Li alloy can improve its discharging current density.

The electrochemical impedance spectra of Mg–8Li–0.5Y and Mg–8Li–1Y electrodes at the open circuit potential in 0.7 mol L^{-1} NaCl solution are shown in Fig. 4. It was used to qualitatively compare the discharge behavior of the two magnesium alloy samples. Both samples show a single capacitive arc at high frequency region. The R_p for Mg–8Li–0.5Y electrode (ca. 383 Ω cm^{-2}) is larger than that for Mg–8Li–1Y electrode (ca. 315 Ω cm^{-2}), indicating that Mg–8Li–1Y electrode is more active than that of Mg–8Li–0.5Y electrode, which is in agreement with the results from current–time measurements.

Fig. 5a and b shows the SEM micrographs of Mg–8Li–0.5Y and Mg–8Li–1Y electrodes, respectively. The images were taken after the samples were consecutively discharged at −1.4, −1.2, −1.0

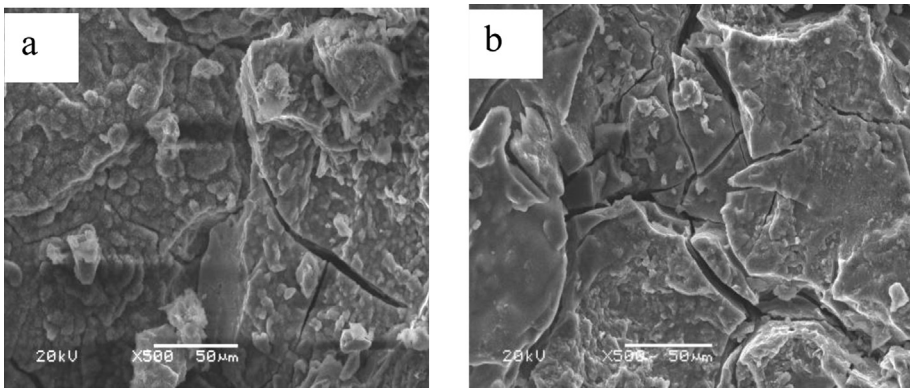

Fig. 5. SEM micrographs of (a) Mg–8Li–0.5Y and (b) Mg–8Li–1Y alloys obtained after the samples were consecutively discharged at −1.4, −1.2, −1.0 and −0.8 V each for 15 min in 0.7 mol L^{-1} NaCl solution.

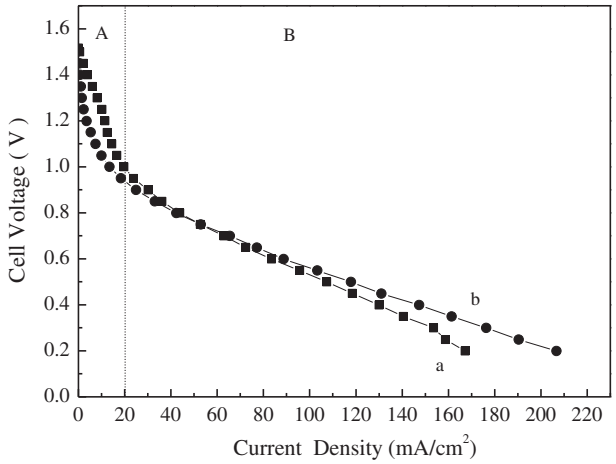

Fig. 6. The plots of the current density vs. cell voltage for the Mg–H_2O_2 semi-fuel cell with (a) Mg–8Li–0.5Y and (b) Mg–8Li–1Y anodes at room temperature. Anolyte: 0.7 mol L^{-1} NaCl. Catholyte: 0.7 mol L^{-1} NaCl + 0.5 mol L^{-1} H_2O_2 + 0.1 mol L^{-1} H_2SO_4. Flow rate: 85 mL min^{-1}.

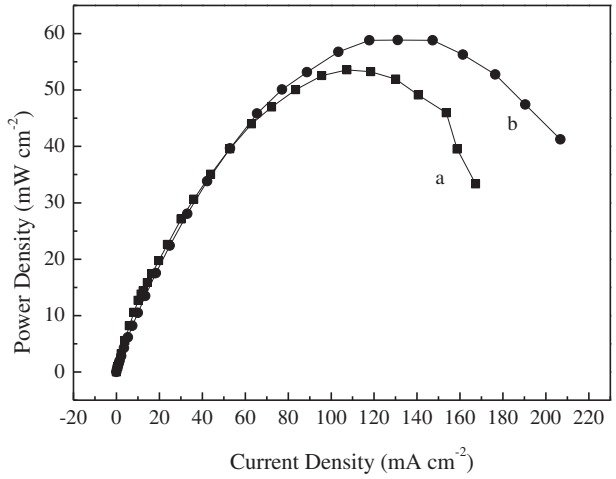

Fig. 7. The plots of the current density vs. power density for the Mg–H_2O_2 semi-fuel cell with (a) Mg–8Li–0.5Y and (b) Mg–8Li–1Y anodes at room temperature. Anolyte: 0.7 mol L^{-1} NaCl. Catholyte: 0.7 mol L^{-1} NaCl + 0.5 mol L^{-1} H_2O_2 + 0.1 mol L^{-1} H_2SO_4. Flow rate: 85 mL min^{-1}.

and −0.8 V each for 15 min in 0.7 mol L^{-1} NaCl solution. Fig. 5a indicated that the oxidation products of Mg–8Li–0.5Y electrode formed thick and large microblocks on the surface. Fig. 5b demonstrated that the Mg–8Li–1Y electrode surface displays deeper and larger channels. These channels allow the electrolyte to penetrate through more easily. As a result, Mg–8Li–1Y electrode has higher discharging currents than Mg–8Li–0.5Y electrode.

3.3. Fuel cell performance

Mg–H_2O_2 semi-fuel cells were assembled using Mg–8Li–0.5Y and Mg–8Li–1Y as the anode, respectively, and their performances were shown in Figs. 6 and 7. Fig. 6 displays the plots of cell voltage versus current density. It can be seen from the two curves that the cell voltage declined rapidly with the increase of current density in the stage of A, implying that the loss of voltage is mainly caused by the activation polarization. However, the voltages of both cells decay nearly linearly with the increase of current density at stage B, demonstrating that the cell performance shows a strong dependence on the ohmic resistance of the cell. The Mg–8Li–1Y anode exhibited better performance than that of Mg–8Li–0.5Y anode, especially at higher current density (>60 mA cm^{-2}). Fig. 7 shows the plots of the power density versus current density. The peak power density of the semi-fuel cell with Mg–8Li–1Y anode is 59 mW cm^{-2}, which is higher than that with Mg–8Li–0.5Y anode (53 mW cm^{-2}), indicating that Mg–8Li–1Y alloy displays better performances than that of Mg–8Li–0.5Y alloy as the anode of Mg–H_2O_2 semi-fuel cells.

4. Conclusions

Casting ingots of Mg–8Li–0.5Y and Mg–8Li–1Y alloys were prepared by the induction melting method and their electrochemical performances in 0.7 mol L^{-1} NaCl solution were studied. Their properties as anode material of Mg–H_2O_2 semi-fuel cells were also investigated.

(1) The Mg–8Li–1Y electrode is more corrosion resistant than Mg–8Li–0.5Y electrode.
(2) The Mg–8Li–1Y electrode has higher discharge activity and peak power density as the anode of Mg–H_2O_2 semi-fuel cells than Mg–8Li–0.5Y electrode.
(3) The Mg–8Li–0.5Y and Mg–8Li–1Y alloys would be the more excellent anodes than Mg in Mg–H_2O_2 semi-fuel cells and may lead to a new research area on the Mg–H_2O_2 semi-fuel cells from both the commercial and fundamental aspects.
(4) Modifying the Y content can alter the performance of the Mg–Li–Y alloy as the anode material of Mg–H_2O_2 semi-fuel cells.

Acknowledgments

This work was financially supported by the National Natural Science Foundation of China (21203040), the Natural Science Foundation of Heilongjiang Province of China (B201201) and the Fundamental Research Funds for the Central Universities (HEUCF201210010) and the Specialized Research Fund for the Doctoral Program of Higher Education (20102304110001).

References

[1] E.G. Dow, R.R. Bessette, M.G. Medeiros, H. Meunier, G.L. Seebach, J. Van Zee, C. Marsh-Omdorff, J. Power Sources 65 (1997) 207.
[2] M.G. Medeiros, R.R. Bessette, C.M. Deschenes, C.J. Patrissi, L.G. Carreiro, S.P. Tucker, D.W. Atwater, J. Power Sources 136 (2004) 226–231.
[3] R.R. Bessette, M.G. Medeiros, C.J. Patrissi, C.M. Deschenes, C.N. LaFratta, J. Power Sources 96 (2001) 240–244.
[4] R.R. Bessette, J.M. Cichon, D.W. Dischert, E.G. Dow, J. Power Sources 80 (1999) 248–253.
[5] W. Yang, S. Yang, W. Sun, G. Sun, Q. Xin, J. Power Sources 160 (2006) 1420.
[6] W. Yang, S. Yang, W. Sun, G. Sun, Q. Xin, Electrochim. Acta 52 (2006) 9.
[7] D.J. Brodrecht, J.J. Rusek, Appl. Energy 74 (2003) 113–124.
[8] O. Hasvold, N.J. Storkersen, S. Forseth, T. Lian, J. Power Sources 162 (2006) 935.
[9] C.Z. Shu, E.D. Wang, L.H. Jiang, J. Power Sources 208 (2012) 159–164.
[10] L.L. Shi, Y.J. Xu, K. Li, Z.P. Yao, S.Q. Wu, J. Curr. Appl. Phys. 10 (2010) 719–723.
[11] D.X. Cao, L. Wu, Y. Sun, G.L. Wang, Y.Z. Lv, J. Power Sources 177 (2008) 624–630.
[12] D.L. Song, X.Y. Jing, J. Wang, Corros. Sci. 53 (2011) 3651–3656.
[13] D.X. Cao, L. Wu, G.L. Wang, Y.Z. Lv, J. Power Sources 183 (2008) 799–804.
[14] G. Liang, J. Alloys Compd. 370 (2004) 123–128.
[15] D.X. Cao, X. Cao, G.L. Wang, L. Wu, Z.S. Li, J. Solid State Electrochem. 14 (2010) 851–855.
[16] Y.Z. Lv, Y. Xu, D.X. Cao, J. Power Sources 196 (2011) 8809–8814.
[17] Y.Z. Lv, M. Liu, D.X. Cao, J. Power Sources 225 (2013) 124–128.
[18] G. Song, A. Atrens, D. Stjohn, J. Nairn, Y. Li, Corros. Sci. 39 (1997) 855–875.
[19] G. Song, A. Atrens, D.S. John, X. Wu, J. Nairn, Corros. Sci. 39 (1997) 1981–2004.
[20] Y.W. Song, D.Y. Shan, Corros. Sci. 51 (2009) 1087–1094.